Frequency modulated self-oscillation and phase inertia in a synchronized nanowire mechanical resonator

2014 New J. Phys. 16 083009

(http://iopscience.iop.org/1367-2630/16/8/083009)

New Journal of Physics
The open access journal at the forefront of physics
Deutsche Physikalische Gesellschaft DPG | IOP Institute of Physics

Frequency modulated self-oscillation and phase inertia in a synchronized nanowire mechanical resonator

T Barois, S Perisanu, P Vincent, S T Purcell and A Ayari

Institut Lumière Matière, UMR5306 Université Lyon 1-CNRS, Université de Lyon 69622 Villeurbanne cedex, France

Received 7 April 2014, revised 17 June 2014
Accepted for publication 27 June 2014
Published 4 August 2014

New Journal of Physics **16** (2014) 083009

doi:10.1088/1367-2630/16/8/083009

Abstract

Synchronization has been reported for a wide range of self-oscillating systems. However, even though it has been predicted theoretically for several decades, the experimental realization of phase self-oscillation, sometimes called phase trapping, in the high driving regime has been studied only recently. We explored in detail the phase dynamics in a synchronized field emission SiC nanoelectromechanical system with intrinsic feedback. A richer variety of phase behavior has been unambiguously identified, implying phase modulation and inertia. This synchronization regime is expected to have implications for the comprehension of the dynamics of interacting self-oscillating networks and for the generation of frequency modulated signals at the nanoscale.

S Online supplementary data available from stacks.iop.org/njp/16/083009/mmedia

Keywords: field emission, nanomechanics, nanowire

A nanoelectromechanical system (NEMS) can be defined as a mobile electrical device at the nanoscale [1] capable of ultrasensitive mass detection [2]. It has been shown that nonlinearities [3] play a major role in such devices [4, 5]. Self-oscillating NEMSs have been recently fabricated and use either an external feedback loop [6] or an intrinsic nanoscale active

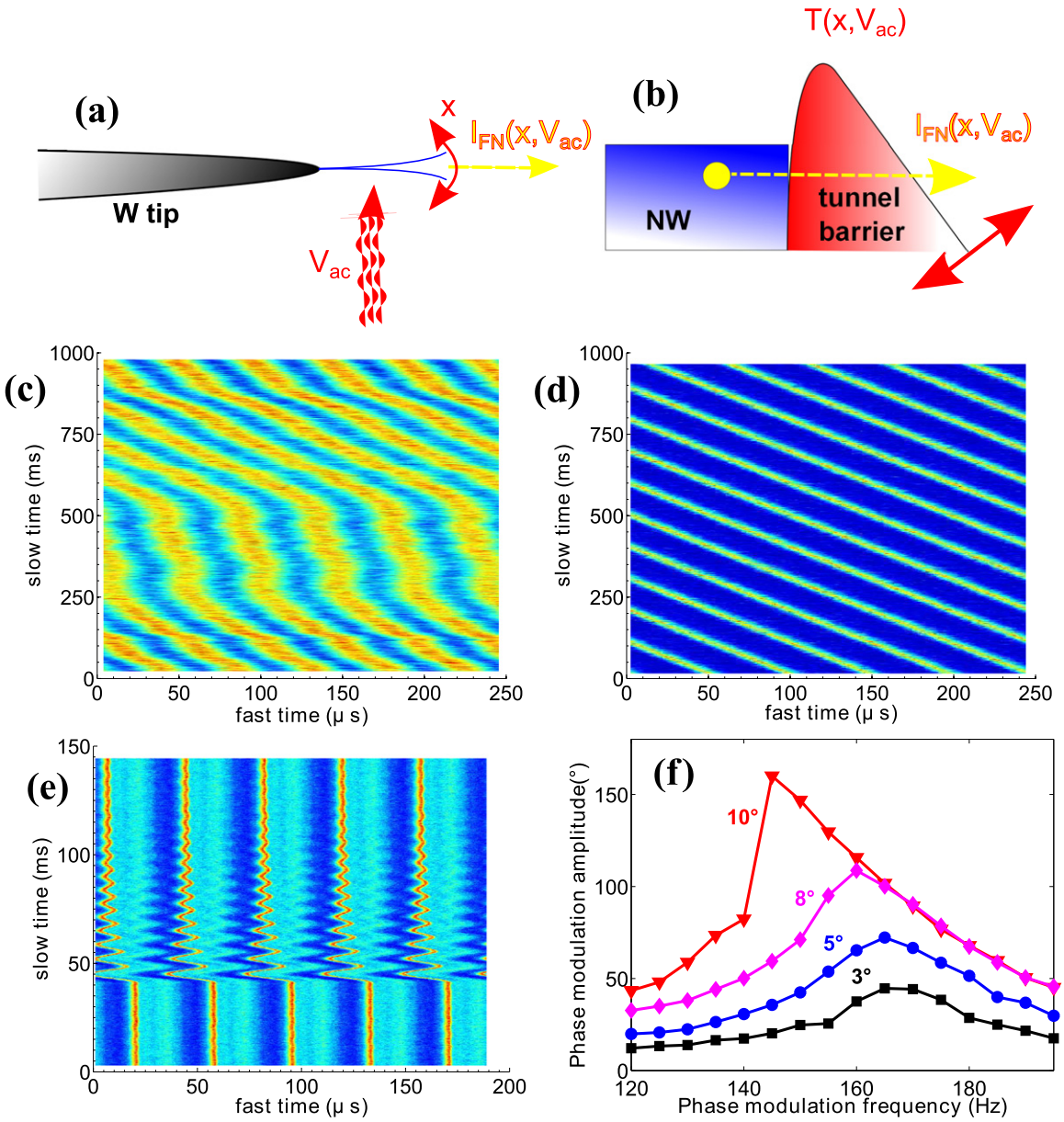

Figure 1. (a) Schematic of a vibrating field emitting NW on a tungsten tip submitted to an AC voltage V_{AC}. (b) Schematic of the tunneling barrier at the NW apex. (c) Temporal map of the field emission current for sample NW1 in the SO regime for $V_{AC} = 0$ V. The oscillating current is in arbitrary units and the colorscale is such that blue denotes low current and red denotes high current. The averaged current is 600 pA and the amplitude of current oscillations is in the 100 pA range. (d) Field emission current temporal map for sample NW2 in the synchronized regime for $V_{AC} = 5$ V and f = 20.8 kHz. The averaged current is 500 pA and the amplitude of current oscillations is in the 100 pA range. (e) Field emission current temporal map for sample NW1 in the synchronized regime for a driving amplitude $V_{AC} = 300$ mV, a driving frequency $f_d = 30.9$ kHz and a 120° phase jump of the driving after 40 ms. A fit of the relaxation time gives 22.5 ms and an oscillation frequency of the phase of 150.3 Hz. The averaged current is 3.15 nA and the amplitude of current oscillations is in the 100 pA range. The asymmetry of the current is related to nonlinear terms that will be neglected in the rest of the article. (f) Experimental vibration amplitude of the phase of the driven SO as a function of the phase modulation frequency $\omega_e/2\pi$ for frequency modulation amplitudes ranging from 3 to 10° for NW1.

mechanism [7–13]. A self-oscillator (SO) is characterized at the first level by a limit cycle, but its most distinguishing feature is the degree of freedom of its phase, which has a zero Lyapunov exponent. The phase can take on any value. Furthermore, contrary to a forced resonator, a forced SO can keep its phase liberty or enter a synchronized regime depending on the synchronization signal. Synchronization is only possible in systems demonstrating self-oscillations.

Synchronization [14, 15], or phase locking, appears in a large variety of systems, such as neural networks, lasers, charge density waves, Josephson junction arrays, heart/breathing systems, and population of flashing fireflies, and it is expected to be exploited for the treatment of Parkinson's disease, signal processing or optomechanical systems [16, 17]. Recently, synchronization has been demonstrated experimentally in NEMSs [18, 19]. A NEMS often operates in a high driving regime due to its size. In this regime, synchronization experiments in lasers [20], hydrodynamics [21] and thermoacoustic oscillators [22] showed an intriguing phase behavior, never observed previously, called phase trapping [23]. In this paper, the full spectrum of behavior of the phase in the high driving regime is discussed, including phase trapping, thanks to the high phase sensitivity of our self-oscillating nanowires (NWs). We define the range in which the generation of phase-modulated signals is possible and show that the power spectrum density (PSD) is not the most appropriate tool for defining the boundary between each regime.

We studied three different SiC self-oscillating nanocantilevers (samples NW1, length L=198 μm, radius r = 160 nm; NW2, L = 90 μm, r = 100 nm; NW3, L = 220 μm, r = 115 nm) fixed at one end to tungsten rigid tips and submitted to AC and DC external electrostatic forces (figure 1(a)). The measurements were performed in an ultra high vacuum chamber equipped with an SEM column and piezoinertial nanomanipulators to position the sample in front of a counterelectrode at a submicron distance. The motion of the NW is transduced into the current because of the dependence of the field emission current on the sample to the counterelectrode distance (for strong amplitude, current rectification by the motion can be visible). The current is collected by a secondary electron detector and recorded on a fast digital oscilloscope. The DC voltage generates a strong electric field at the free end of the NW, allowing conduction electrons to tunnel into the vacuum through the field emission triangular barrier. Local electric field variations at the NW apex modulates the transparency of the barrier (figure 1(b)). Their origin can be from geometrical changes, such as the mechanical displacement of the NW free end, as well as from modulated power supplies that induce changes in the voltage on the NW. An intrinsic feedback loop is created because a tiny fluctuation of the position of the NW end changes the transparency of the barrier and the tunneling current, which in turns changes the voltage drop along the NW and the voltage at the apex. The voltage changes modify the transparency of the barrier and the electrostatic force on the NW and thus, induce a counterreaction on the NW position. This generates self-oscillation at a frequency close to the original resonant frequency of the mechanical resonator [24].

Figures 1(c), (d) and (e) are measurements of the field emission current amplitude in the self-oscillation regime as a function of two time scales [25, 26]. The maps are obtained as follows: for a fixed V_{DC}, the field emission current is recorded for a time between 0.2 and 1 s, depending on the experimental run. The first line of the map is the signal from the beginning to a fixed time τ, where τ is chosen such that a few oscillation periods are visible on this line. The intensity of the current is represented in colorscale. The second line of the map represents the signal just after τ up to 2 τ and the rest of the map is built in the same manner. In the absence of

phase drift, straight lines of the same color are expected. The angle of these lines depends on the oscillation period and τ.

In figure 1(c) when no AC signal is applied, on the short time scale (i.e., x-axis) the signal appears periodic; however, on the long time scale (i.e., y-axis) it can be seen that the phase has no preferred value and drifts freely like a Brownian particle. When an AC voltage is applied with frequency close to the self-oscillating frequency, the SO is locked and the phase is stabilized (figure 1(d)) as can be seen from the straight lines. Actually, the phase still drifts due to the intrinsic drift of the AC generator, but on a much longer time scale which is not visible here.

Synchronization results from the competition between the natural frequency of a SO and the frequency of an external drive. If the external frequency is sufficiently close to the self-oscillation frequency, the SO is entrained by the external drive. In this synchronized region, the self-oscillation frequency disappears. Out of the synchronized region, both frequencies coexist and the system is said to be quasiperiodic [27, 28]. The dynamics of the phase and amplitude of an individual SO in the simplest case are governed by a first-order time derivative and thus, by nature are overdamped [24]. For an abrupt change of the generator phase, the phase of the SO should relax exponentially to a new phase value that maches the generator phase, similar to an overdamped particle (OP) relaxing to a potential minimum. Figure 1(e) shows damped oscillations of the phase toward its new fixed value. The phase itself behaves like a resonator. We term this the phase inertia (PI) regime. The open-loop relaxation time is of the order of 170 ms, the closed-loop relaxation time is of the order of 800 ms, and the detuning frequency is of about 1 kHz; these do not match with the oscillation frequency of the phase of 175 Hz, nor the phase relaxation time around several tens of ms. A resonance curve of the phase can be performed if a frequency modulated signal $\varphi_e(t) = \delta\theta \cos(\omega_e t)$ is applied to the NW where $\delta\theta$ is the frequency modulation amplitude and ω_e is the swept angular frequency modulation of the phase. Figure 1(f) is a plot of resonance curves of the phase for different $\delta\theta$. For high forcing $\delta\theta$, the resonance curves shows Duffing nonlinearities. For higher forcing, the phase unlocks when its amplitude is above 180° and we didn't observe a partly entrained regime. The Duffing nonlinearities comes from the cos (φ) term in the phase equation (see supporting information, available from stacks.iop.org/njp/16/083009/mmedia). This behavior is observed for a strong AC driving, inducing nonlinear oscillations of our samples and a large detuning (i.e., difference between the driving and the NW resonant frequencies). The detuning can typically be up to a few percent of the resonant frequency.

This regime of self-oscillation under strong driving and detuning was explored in more detail and four main dynamical behaviors were observed, which are summarized in figure 2. Outside the synchronization region, for a high enough detuning, the phase difference between the drive and the field emission oscillating current increases quasi-linearly (figure 2(a)) and the slope is given by the detuning, which is as expected for an unlocked SO regime. The phase has no preferred value, as observed in the probability density function (PDF) and only 1/f noise appears in the PSD. For low detuning, the phase is locked and fluctuates around an average value, with fluctuations lower than 2π, as seen in figure 2(d). This is the OP regime mentioned previously and the PSD is similar in shape but smaller in amplitude than for the SO regime. When the detuning is increased, the phase still has Gaussian amplitude fluctuations (figure 2(c)) around a fixed value, similar to the OP regime; however, these fluctuations occur with a nonzero average frequency, as observed in the PSD. This is the PI regime. Finally, for a higher detuning, before unlocking, the system can reach a phase-modulated regime where the phase enters self-

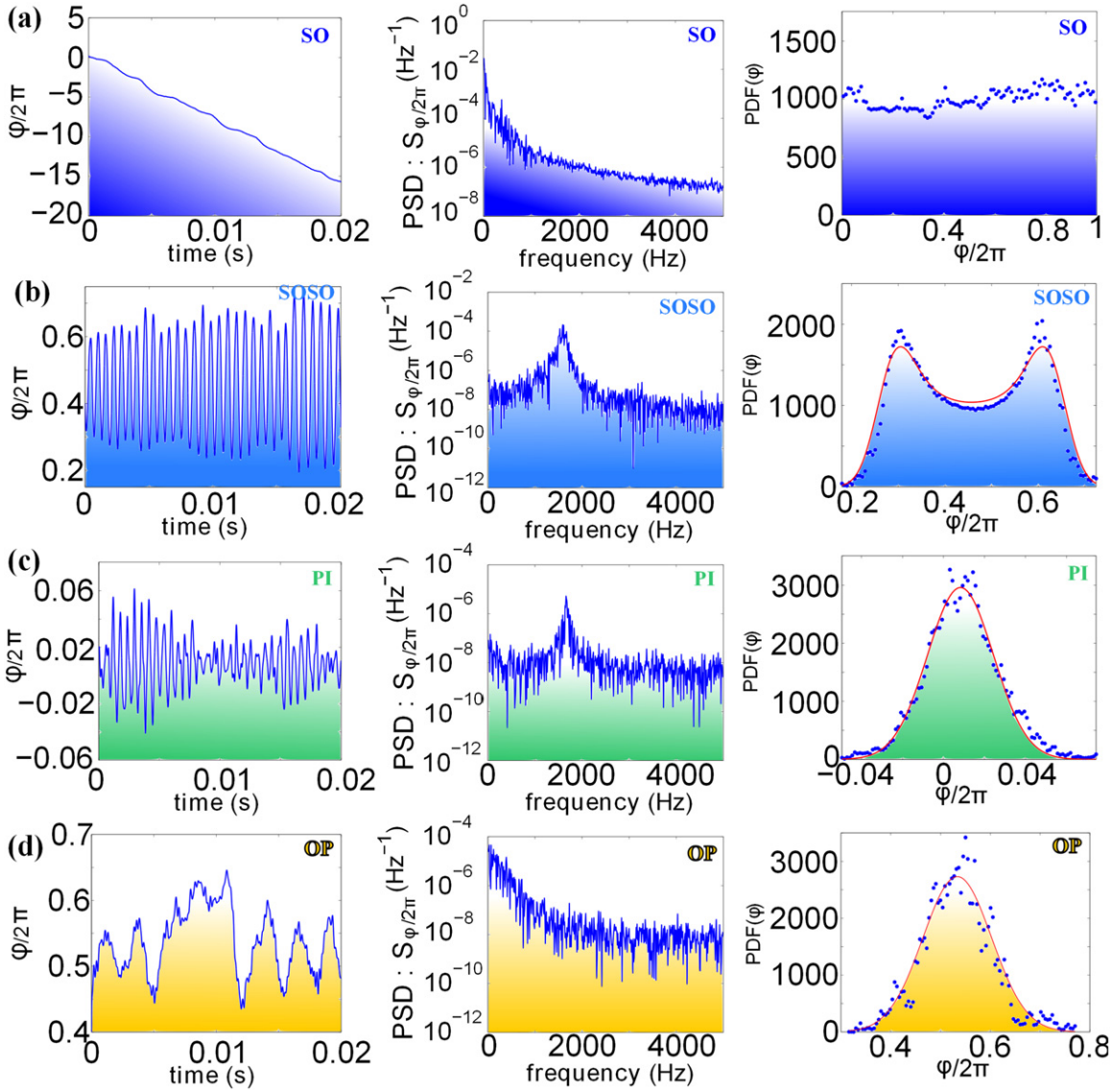

Figure 2. Experimental signature of the phase dynamics in the SO, SOSO, PI and OP regimes for NW2, (left) time dependence of the phase, (middle) semilog plot of the PSD of the phase and (right) PDF of the phase. (a) SO regime for $V_{AC} = 0.1$ V and a detuning of 1 kHz. (b) SOSO for $V_{AC} = 5.9$ V and a detuning of −3 kHz. (c) PI regime for $V_{AC} = 6.1$ V and a detuning of −1 kHz. (d) OP regime for $V_{AC} = 0.4$ V and a detuning of 0 kHz.

oscillation itself. This regime is called phase trapping [23] or imperfect phase locking [22]. In the following, we refer to it as self-oscillating self-oscillation (SOSO). The amplitude of phase oscillations in the SOSO regime is roughly constant, as observed in figure 2(b), and of fixed frequency.

Distinguishing between the SOSO, PI, and SO regimes is experimentally challenging because of noise. Perhaps this is why the PI has not been observed in the past. The lack of information in the literature makes it difficult to compare our noise amplitude with the amplitude of other experiments. Indeed, noise can induce important amplitude fluctuations in

the SOSO regime that render the signal for low amplitude of phase self-oscillation similar to the PI regime. When the amplitude of phase self-oscillation becomes large enough to be above the noise level, it may become greater than 2π, which leads to phase unlocking similar to the SO regime. For instance, in [20], the authors, observed an enlargement of the phase PDF and interpreted it as the first observation of frequency locking without phase locking; however, other interpretations are possible. An increase of the width could also be related to chaotic behavior, increased noise in the PI state, a softening of the restoring force of the phase, or phase slips (see supporting information). In figure 2(b), a clear signature of SOSO is shown with a typical two peak PDF shape, indicating that the phase is oscillating with a rather constant amplitude. The PSD itself can not distinguish between the different phase regime.

These four behaviors are generic of a strongly driven SO and can theoretically be obtained even from a simple driven Van der Pol oscillator [14, 15] (see supporting information, available from stacks.iop.org/njp/16/083009/mmedia):

$$m\ddot{x} + m\lambda\dot{x} + m\gamma\dot{x}x^2 + m\omega_0^2 x = Fcos(\omega_d t) \tag{1}$$

where m is the effective mass of the nanocantilever, x the displacement of the nanocantilever tip in the transverse direction, the dot refers to the derivative versus time t, λ is the linear negative damping, γ is the nonlinear damping coefficient responsible for the limit cycle, $\omega_0/2\pi$ is the natural frequency of the resonator, F the electrostatic force, and $\omega_d/2\pi$ is the frequency of the external driving. The driven SO position is given by $x(t) = R\cos(\omega_d t - \varphi)$, where R is the amplitude of self-oscillation and φ is its phase. Here, $R(t)$ and $\varphi(t)$ are the two slowly varying degrees of freedom compared to the period of the SO. From equation (1), the amplitude and phase dynamical equations can be deduced:

$$R_0\dot{\tilde{\varphi}} = \delta\omega\tilde{R} + \frac{1}{2}\left(-\lambda - \frac{\gamma}{4}R_0^2\right)R_0\tilde{\varphi} \tag{2}$$

$$\dot{\tilde{R}} = \frac{1}{2}\left(-\lambda - \frac{3\gamma}{4}R_0^2\right)\tilde{R} - \delta\omega R_0\tilde{\varphi} \tag{3}$$

where $\delta\omega = (\omega_d^2 - \omega_0^2)/2\omega_d$ can be assimilated to the detuning frequency. Here, R_0 is the self-oscillation amplitude, $\tilde{\varphi}$ is a small perturbation around the equilibrium phase, and $\tilde{R}$ is a small perturbation around R_0 (the equilibrium phase and amplitude value can be obtained from the equations given in the supporting information). After some algebra, the phase and amplitude dynamical equations provide the linear equation for the phase:

$$\dddot{\tilde{\varphi}} + \Gamma\ddot{\tilde{\varphi}} + \Omega^2\dot{\varphi} = 0 \tag{4}$$

where $\Gamma = \lambda + \frac{\gamma}{2}R_0^2$ and $\Omega^2 = \frac{1}{4}[(\lambda + \frac{3\gamma}{4}R_0^2)(\lambda + \frac{\gamma}{4}R_0^2) + 4\delta\omega^2]$. From this equation, we determine the OP regime for low detuning and the PI regime for higher detuning. For even higher detuning, R_0 can decrease enough that the damping Γ becomes negative, thus reaching the SOSO regime. Nonlinear terms can be added to this equation to model the SOSO to SO transition [15] (see supporting information). This model predicts that for high detuning, the phase oscillation frequency Ω is independent of the forcing amplitude and is equal to the detuning.

We performed a detuning amplitude mapping of the synchronization region. In figure 3(a), a point in the map is considered in the SO regime if the phase is not bounded, in the SOSO regime if the PDF of the phase has two peaks, in the PI regime if the PSD has a peak for any frequency other than zero, and if the PDF of the phase has a single peak. If a point on the map

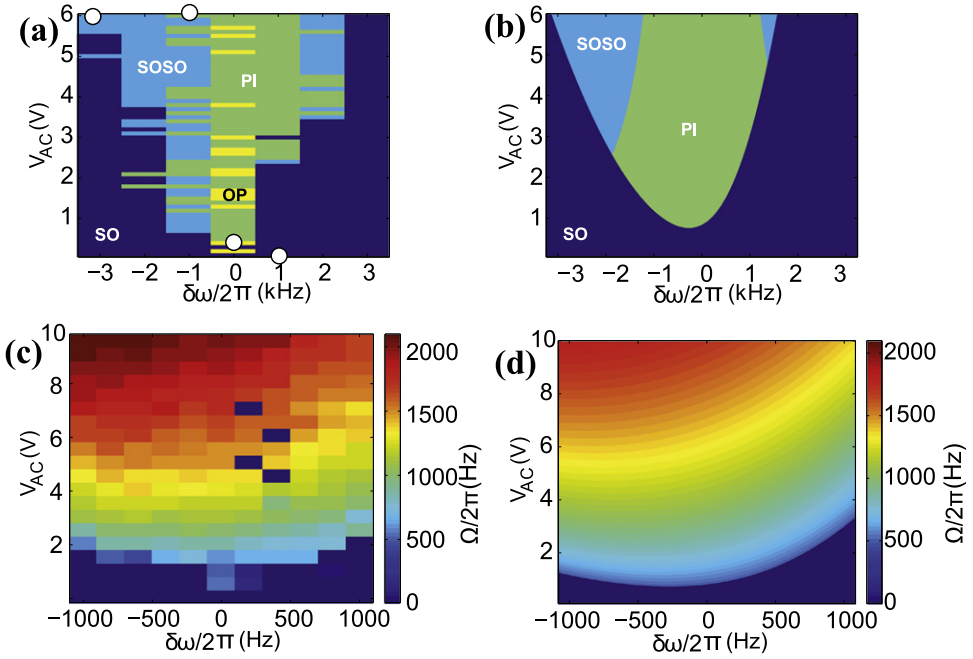

Figure 3. (a) Experimental frequency amplitude mapping (i.e., Arnold tongue) of the different synchronization regime for NW2. The white dots correspond to the experimental points of figure 2. Dark blue denotes the SO regime, light blue denotes the SOSO regime, green denotes the PI regime, and yellow denotes the OP regime. (b) Simulated frequency amplitude mapping of the different synchronization regime. (c) Experimental frequency amplitude mapping of the phase frequency $\Omega/2\pi$ in the PI region for the same experimental conditions as in (a). (d) Simulated frequency amplitude mapping of the phase frequency $\Omega/2\pi$ in the PI region.

does not meet these conditions, it is considered in the OP regime. In figure 3(c), the phase frequencies are extracted from the maximum of the phase PSD. Because of fluctuations, the exact frontier of the Arnold tongue [14, 15] may vary, but the four regimes are always present when the measurement is repeated and therefore SOSO regime always appears for high forcing and detuning. The points marked as OP may be either true OP states or, more likely, are PI states with an amplitude of the 1/f noise dominating the oscillation frequency. In addition to the existence of a large SOSO region, the most remarkable feature of this tongue is the behavior of the phase frequency (figure 3(c)). This frequency is strongly dependent on the forcing amplitude and is different from the detuning frequency contrary to the preceding Van der Pol model predictions. Thus, it is not directly related to frequency beating between the two main signals. We developed a phenomenological model to explain this behavior by adding nonlinear dependencies of the damping and the frequency in the Van der Pol model. Here, ω_0 is replaced in equation (1) by $\omega_t^2 = \omega_0^2 + \mu^*(\omega_d^2 - \omega_0^2)x^2 + \nu\sqrt{F}$, where ν is a negative constant that considers the fact that the maximum of the phase frequency shift toward negative detuning for increasing F and $\mu^* = \mu/R_0^2$ is such that this term is less effective for high self-oscillation amplitude R_0. The physical origin of such nonlinearities could be the strong electrostatic frequency tuning of nanocantilevers during field emission [29] and the nonlinear intrinsic feedback between the electrical circuit and mechanical motion [7, 30]. The nonlinearities of the field emission current down mixes the driving voltage and the self-oscillation signal (the term

$\omega_d^2 - \omega_0^2 \approx 2(\omega_d - \omega_0)\omega_0$ is proportional to the detuning). This mixed signal is then transmitted to the apex voltage because of the voltage drop across the NW, which in turns modifies the tuning frequency. If the electrical circuit has an in-phase back action on the mechanical motion, it will have also an out-of-phase effect and the damping will also be affected. This implies that the damping should have an expression of the form $\lambda = \lambda_0 + \lambda_1 F(\omega_d - \omega_0)^2$, where λ_0 and λ_1 are constant. This model gives a very good agreement with experimental data (figures 3(b)–(d)).

In conclusion, we have observed experimentally low, and even negative, friction phase motion in a field emission NEMS. We found that the phase itself has a resonant frequency when driven at high amplitude and can SO for high mismatch between the SO frequency and the driving frequency. In principle, synchronization of the self-oscillating phase and even observation of a self-oscillation of the phase of the self-oscillating phase should be possible. In our experiment, this regime was too unstable, as this would require additional phase motion in a region near to the desynchronization limit. However, such a phenomenon may be observable by working at low temperature, which would considerably reducing the phase noise. Although NEMSs, and this system in particular, are not mature enough for radio communication applications, the SOSO regime could be an original way of generating frequency modulated signals to obtain better data transmission [31] and signal processing. This work was limited to the study of a single SO in the high driving limit but SOSO, which was challenging to observe previously in isolated oscillators, might be an interesting phenomenon to study in the dynamics of multiple coupled SOs in the strong coupling limit. The Adler equation [32] and the Kuramoto model [33] are widely used to describe the dynamics of synchronized systems but only consider the phase degree of freedom. Phase resonance and phase self-oscillation can be theoretically introduced into the Kuramoto framework by inserting phenomenological inertial terms and phase delay between several SOs [34]. However, strong coupling is assumed, which is incompatible with the Kuramoto model [35]. In strongly nonlinear self-oscillating systems, such as NEMSs the phase and amplitude are coupled and the Adler equation or the Kuramoto model are no longer valid. In particular, multiple self-oscillating field emission NEMSs coupled electrostatically could be an interesting system to study the transition from locking to the unsteady regime of synchronization with Hopf oscillation and then amplitude death, as predicted in [36] for coupled SOs.

Acknowledgments

The authors acknowledge the ‘Plateforme Nanofils et Nanotubes Lyonnaise’ of the University Lyon1. This work was supported by the Région Rhône-Alpes (PROGRAMME SRESR—CIBLE 2008 and cluster MACODEV) and the French National Research Agency (ANR) through its Nanoscience and Nanotechnology Program (NEXTNEMS, ANR-07-NANO-008–01 and NEMSPiezo, ANR-08-P078–48-03) and Jeunes Chercheuses et Jeunes Chercheurs Program (AUTONOME, ANR-07-JCJC-0145–01).

References

[1] Craighead H G 2000 *Science* **290** 1532
[2] Chaste J, Eichler A, Moser J, Ceballos G, Rurali R and Bachtold A 2012 *Nature Nanotechnol.* **7** 301

[3] Lifshitz R and Cross M 2008 *Reviews of Nonlinear Dynamics and Complexity* vol 1 ed H G Schuster (Weinheim: Wiley-VCH) p 1

[4] Perisanu S, Barois T, Ayari A, Poncharal P, Choueib M, Purcell S T and Vincent P 2010 *Phys. Rev.* B **81** 165440

[5] Eichler A, Moser J, Chaste J, Zdrojek M, Wilson-Rae I and Bachtold A 2011 *Nat. Nanotechnol.* **6** 339

[6] Kawakatsu H, Kawai S, Saya D, Nagashio M, Kobayashi D, Toshiyoshi H and Fujita H 2002 *Rev. Sci. Instrum.* **73** 2317

[7] Ayari A, Vincent P, Perisanu S, Choueib M, Gouttenoire V, Bechelany M, Cornu D and Purcell S T 2007 *Nano Lett.* **7** 2252

[8] Steeneken P G, le Phan K, Goossens M J, Koops G E J, Brom G J A M, van der Avoort C and van Beek J T M 2011 *Nat. Phys.* **7** 354

[9] Grogg D, Ayoz S and Ionescu A 2009 *IEEE International Electron Devices Meeting (IEDM) 2009* pp 1–4

[10] Koenig D R and Weig E M 2012 *Appl. Phys. Lett.* **101** 213111

[11] Aubin K, Zalalutdinov M, Alan T, Reichenbach R, Rand R, Zehnder A, Parpia J and Craighead H 2004 *J. Microelectromech. Syst.* **13** 1018

[12] Vincent P, Perisanu S, Ayari A, Choueib M, Gouttenoire V, Bechelany M, Brioude A, Cornu D and Purcell S T 2007 *Phys. Rev.* B **76** 085435

[13] Kleshch V I, Obraztsov A N and Obraztsova E D 2009 *JETP Lett.* **90** 464–8

[14] Pikovsky A, Rosenblum M and Kurths J 2003 *Synchronization: A Universal Concept in Nonlinear Sciences* (*Cambridge Nonlinear Science Series*) (Cambridge: Cambridge University Press)

[15] Balanov A, Janson N and Postnov D 2008 *Synchronization: From Simple to Complex* (Berlin: Springer)

[16] Zhang M, Wiederhecker G S, Manipatruni S, Barnard A, McEuen P and Lipson M 2012 *Phys. Rev. Lett.* **109** 233906

[17] Marquardt F, Harris J G E and Girvin S M 2006 *Phys. Rev. Lett.* **96** 103901

[18] Barois T, Perisanu S, Poncharal P, Vincent P, Purcell S and Ayari A 2012 *Int. Conf. on Electromagnetics in Advanced Applications (ICEAA) 2012* pp 551–3

[19] Matheny M H, Grau M, Villanueva L G, Karabalin R B, Cross M and Roukes M L 2014 *Phys. Rev. Lett.* **112** 014101

[20] Thévenin J, Romanelli M, Vallet M, Brunel M and Erneux T 2011 *Phys. Rev. Lett.* **107** 104101

[21] Li L K B and Juniper M P 2013 *J. Fluid Mech.* **735** R5

[22] Penelet G and Biwa T 2013 *Am. J. Phys.* **81** 290

[23] Aronson D, Ermentrout G and Kopell N 1990 *Physica D: Nonlinear Phenomena* **41** 403

[24] Barois T, Perisanu S, Vincent P, Purcell S T and Ayari A 2013 *Phys. Rev.* B **88** 195428

[25] Giacomelli G and Politi A 1996 *Phys. Rev. Lett.* **76** 2686

[26] Arecchi F T, Giacomelli G, Lapucci A and Meucci R 1992 *Phys. Rev.* A **45** R4225

[27] Hohl A, Gavrielides A, Erneux T and Kovanis V 1999 *Phys. Rev.* A **59** 3941

[28] Libchaber J and Glazier A 1988 *IEEE Trans. Circuits Syst.* **35** 790

[29] Purcell S T, Vincent P, Journet C and Binh V T 2002 *Phys. Rev. Lett.* **89** 276103

[30] Lazarus A, Barois T, Perisanu S, Poncharal P, Manneville P, de Langre E, Purcell S T, Vincent P and Ayari A 2010 *Appl. Phys. Lett.* **96** 193114

[31] Gouttenoire V, Barois T, Perisanu S, Leclercq J L, Purcell S T, Vincent P and Ayari A 2010 *Small* **6** 1060–5

[32] Adler R 1946 *Proc. IRE* **34** 351

[33] Kuramoto Y 2003 *Chemical Oscillations, Waves and Turbulence* (*Dover Books on Chemistry Series*) (New York: Dover)

[34] Hong H, Jeon G S and Choi M Y 2002 *Phys. Rev.* E **65** 026208

[35] Acebrón J A, Bonilla L L, Pérez Vicente C J, Ritort F and Spigler R 2005 *Rev. Mod. Phys.* **77** 137

[36] Matthews P C and Strogatz S H 1990 *Phys. Rev. Lett.* **65**